Water Adsorption, Desorption, and Clustering on FeO(111)

John L. Daschbach,[†] Z. Dohnálek,[‡] Shu-Rong Liu,[‡] R. Scott Smith,[‡] and Bruce D. Kay*[,‡]

Environmental Molecular Sciences Laboratory, Fundamental Science Division, Pacific Northwest National Laboratory, PO Box 999, Mail Stop K8-88, Richland, Washington 99352

Received: January 12, 2005; In Final Form: March 18, 2005

The adsorption of water on FeO(111) is investigated using temperature programmed desorption (TPD) and infrared reflection absorption spectroscopy (IRAS). Well-ordered 2 ML thick FeO(111) films are grown epitaxially on a Pt(111) substrate. Water adsorbs molecularly on FeO(111) and desorbs with a well resolved monolayer peak. IRAS measurements as a function of coverage are performed for water deposited at 30 and 135 K. For all coverages (0.2 ML and greater), the adsorbed water exhibits significant hydrogen bonding. Differences in IRAS spectra for water adsorbed at 30 and 135 K are subtle but suggest that water adsorbed at 135 K is well ordered. Monolayer nitrogen TPD spectra from water covered FeO(111) surfaces are used to investigate the clustering of the water as a function of deposition or annealing temperature. Temperature dependent water overlayer structures result from differences in water diffusion rates on bare FeO(111) and on water adsorbed on FeO(111). Features in the nitrogen TPD spectra allow the monolayer wetting and 2-dimensional (2D) ordering of water on FeO(111) to be followed. Voids in a partially disordered first water layer exist for water deposited below 120 K and ordered 2D islands are found when depositing water above 120 K.

I. Introduction

In nature metal oxide surfaces predominate over pristine metal surfaces. In contrast, the vacuum surface science literature is more abundant for the latter. This is in large part a manifestation of the relative difficulty in preparing highly reproducible, clean surfaces of oxides. A powerful technique enabling the production of high quality metal oxide surfaces is to grow epitaxial thin films of an oxide on a substrate of different composition. Most commonly, the substrate is a metal with a good lattice match to the desired oxide overlayer. In general, the electronic structure of oxide overlayers has been found to converge to the bulk oxide structure for films 2−3 monolayers (ML) thick or greater.[1−3] There are numerous good reviews on this subject.[4−8]

Metal oxides are important from both a fundamental and practical perspective. Their ubiquity in nature provides an impetus to study these materials from a fundamental standpoint. The widespread use of metal oxides in catalytic and environmental applications motivates practical interest. Metal oxide catalysts are used in a wide range of industrial chemical production techniques including selective oxidation and dehydrogenation.[9] They are used in environmental cleanup applications to immobilize pollutants or convert them to a more benign form.[9]

Understanding the interactions which determine the reactivity or stability of a metal oxide in a particular environment are aided by detailed studies on reproducibly prepared samples.[7] Iron oxide surfaces are important both in nature and in technological applications and form a class of materials with varied reactivity. Iron oxide thin films including FeO(111), Fe_3O_4(111), and α-Fe_2O_3(0001) have been prepared on Pt(111) and studied by a range of experimental techniques and theoretical methods.[9−14] These include low-energy electron diffraction (LEED),[14,15] high-resolution transmission electron microscopy (HRTEM),[16] X-ray photoelectron diffraction (XPD),[17] and scanning tunneling microscopy (STM).[14,18] Studies focusing on chemical interactions with these surfaces, including the adsorption of water and ethylbenzene, have determined that the reactivity is correlated with the presence of iron atoms at the surface.[19−22] Water is found to dissociate on Fe-terminated Fe_3O_4(111) but not on oxygen-terminated FeO(111).[19,20] In a recent study, we showed that methane (CH_4) and its chlorinated derivatives (CH_3Cl, CH_2Cl_2, $CHCl_3$, and CCl_4) adsorb and desorb from the FeO(111) surface molecularly through a physisorption process.[23]

Of the molecules that have been studied on surfaces, water is likely the most frequently investigated. Because water is a common adsorbate in both natural and technological processes, and because the behavior of adsorbed water is varied, it continues to attract widespread scientific interest.[24,25] An area of vibrant investigation is the processes of water wetting, clustering, and structural ordering on substrates where it adsorbs molecularly. Recent STM studies on Pt(111) and Pd(111) have provided real space images of the way in which water clusters on these surfaces.[26−28] Other experimental and theoretical work has addressed differences from the traditional bilayer model for nondissociative adsorption on Pt(111) and other transition metal surfaces.[29−31]

Water adsorption on FeO(111) has been investigated by TPD, ultraviolet and X-ray photoelectron spectroscopies (UPS, XPS), and IRAS.[9,19,20,32] Using UPS measurements made in adsorption−desorption equilibrium, Joseph et al.[19] concluded that water initially adsorbs as a monomer to a saturation coverage of 4×10^{14} cm^{-2} followed by the formation of a bilayer of water molecules hydrogen bonded to the monomers. A kinetic analysis determined the isosteric heats of adsorption of $q_{st} = 52$ kJ mol^{-1},

* To whom correspondence should be addressed. Phone: (509) 376-0028. Fax: (509) 376-6066. E-mail: Bruce.Kay@pnl.gov.
[†] Environmental Molecular Sciences Laboratory.
[‡] Fundamental Science Division.

10.1021/jp058013s CCC: $30.25
Published on Web 04/21/2005

with a preexponential $\nu = 3 \times 10^{15}$ s^{-1} for the monomers and $q_{st} = 47$ kJ mol^{-1}, $\nu = 3 \times 10^{15}$ s^{-1} for the bilayer. The monomer q_{st} was equated with the desorption activation energy E_a but the authors were unable to resolve the TPD into contributions from monomers and bilayer molecules and unable to determine E_a for the bilayer. Leist et al.[32] determined using IRAS that at 110 K water adsorbed on FeO(111) was hydrogen bonded starting from the lowest coverage studied, 0.1 ML. They interpreted the infrared spectra as resulting from an amorphous deposit formed due to low surface mobility at 110 K.

In this work, we extend the study of water adsorption and clustering on FeO(111) using TPD of both adsorbed water and monolayer nitrogen overlayers, and IRAS at low (30 K) and high (135 K) temperature. Both high quality TPD and IRAS show no evidence of an isolated monomeric species in the water monolayer. The water TPD spectra indicate a monolayer of water wets the FeO(111) surface at the temperature of desorption. The IRAS data show signs of significant hydrogen bonding at coverages as low as 0.2 ML. Water adsorbed on FeO(111) at 135 K shows spectral features interpreted as resulting from an ordered 2D water overlayer, whereas water adsorbed at 30 K appears disordered. In previous work, we have shown that the TPD spectra of physisorbed atoms and molecules can be used to determine the distribution of adsorption sites on oxides and the degree of crystallinity of water overlayers on solid substrates.[33−35] Using nitrogen TPD, we show that wetting of the FeO(111) surface is kinetically limited at low temperatures by the water surface diffusion rates on both the FeO(111) surface and on a layer of adsorbed water. The surface diffusion rate is found to be higher on the FeO(111) surface. We follow the formation and ordering of 2D islands of water on the FeO(111) surface as a function of temperature. Complete 2D ordering of adsorbed water is found only close to onset of measurable desorption. The 2D ordering is more readily distinguished with N_2 TPD than with IRAS. For growth at ~0.5 ML s^{-1} and temperatures >120 K, water forms ordered 2D islands on the surface.

II. Experimental Section

The experiments were performed in an ultrahigh vacuum (UHV) chamber with a base pressure of $\leq 1 \times 10^{-10}$ Torr. The sample substrate was a 1 cm diameter Pt(111) disk, 1 mm thick. The sample was spot-welded to two tantalum wire leads, 2 mm in diameter, clamped in a Au plated Cu jig attached to a closed cycle He cryostat, and resistively heated through the Ta leads. The temperature was monitored with a K-type thermocouple spot welded to the back of the Pt(111) sample and controlled by computer over a range of 28−1300 K. The relative isothermal temperature stability was better than ±0.05 K, and we estimate the error in the absolute temperature to be ±2 K. The surface purity and order of the Pt(111) substrate were checked using Auger electron spectroscopy (AES) and LEED.

Thin FeO(111) films (~2 ML thick) were grown epitaxially on the Pt(111) substrate as described previously.[9,23] Comparison of the LEED pattern and monolayer N_2 desorption with previous work was used to confirm the growth of an epitaxial FeO(111) layer on the Pt(111) substrate. The samples were robust over the temperature range, 28−1000 K, used in this study. The monolayer N_2 TPD line shape characteristic of a clean, well-ordered FeO(111) layer could be regenerated by annealing the sample at 900 K in a partial pressure of 10^{-6} Torr of O_2 for 5 min.

The quasieffusive H_2O (D_2O) beam was produced by expanding the neat vapor at 2.0 Torr through a 1 mm diameter aperture. The N_2 beam was produced by expanding the gas at ~12 Torr through a 0.1 mm diameter aperture. The data reported here were taken with the H_2O (D_2O) beam at 0° and the N_2 beam at 15° with respect to the sample normal. Both beams were quadruply differentially pumped prior to impinging on the FeO(111)/Pt(111) target. Electronically controlled shutters between the beam defining apertures in the second differential pumping stage allowed for control of the water fluence to better than ±0.02 ML. The H_2O beam illuminates a spot on the sample of about 8 mm at normal incidence and the N_2 beam illuminates a spot of about 5 mm centered in the H_2O spot. The H_2O (D_2O) flux was 0.53 ML s^{-1} (0.5 ML s^{-1}). The flux was calibrated using TPD by determining the water exposure time required to saturate the H_2O monolayer layer on Pt(111). Recent STM,[26,36] LEED,[37] and He atom scattering studies[38,39] of the H_2O monolayer on Pt(111) indicate there are a variety of structures of varying density (9.0×10^{14}−1.2×10^{15} cm^{-2}) near saturation of the monolayer, depending on sample temperature and water flux. Ordered 2D structures are found for slow growth conditions, with sample temperatures (135−145 K) and water flux (<0.05 ML s^{-1}). The structure and density of the saturated monolayer in the TPD calibration is not known but probably does not lie outside this range.

The H_2O (D_2O) TPD spectra were acquired using a line-of-sight quadrupole mass spectrometer. The N_2 TPD spectra were acquired with a separate quadrupole mass spectrometer in either an angle-integrated manner or at an angle of 65° with respect to the sample normal. The N_2 TPD line shape was found to be insensitive to the detector position.

Infrared reflection absorption spectra were recorded with a Bruker Equinox 55 Fourier transform spectrometer. The unpolarized infrared beam was focused through a KBr window onto the sample using a BaF_2 lens ($f = 500$ cm), mounted in a nitrogen purged compartment external to the vacuum chamber. The infrared signal was collected in a separate nitrogen purged compartment using a BaF_2 lens ($f = 5$ cm) focused onto a liquid nitrogen cooled MCT detector. Data were collected with the sample at 30 K with a resolution of 4 cm^{-1}. Reference and sample spectra were accumulated for 4000 scans (1000 s.) each. To increase the signal-to-noise ratio, the submonolayer water experiments were repeated between four and eight times and the resulting spectra averaged.

III. Results and Discussion

A. Temperature Programmed Desorption of H_2O and D_2O. Coverage dependent TPD spectra for H_2O (D_2O) desorption from FeO(111) are shown in Figure 1a (Figure 1b). The TPD spectra fill from the high-temperature side as the initial water exposure increases. For an initial water exposure ≤1.0 ML, a single peak with a close to first-order line shape at 166 K (169 K) is found. With higher initial water coverage, a second peak grows in at lower temperature. The higher temperature peak is due to desorption of the first monolayer of water in direct contact with the FeO(111) surface. The lower temperature peak is from water adsorbed on an underlying water layer. The two peak structure is similar to what is observed for water desorption from Pt(111).[37,40] Saturation of the monolayer occurs for the same water exposure as on Pt(111), and therefore, we expect the monolayer density to be nearly identical and equal to $\sim 1 \times 10^{15}$ cm^{-2}.[41] The monolayer and second layer peaks are well resolved, separated by about 11 K for H_2O and 9 K for D_2O. This indicates that water adsorbed on FeO(111) is more strongly bound than water in the layers above and that it wets the FeO(111) surface at the desorption temperature. Spectra

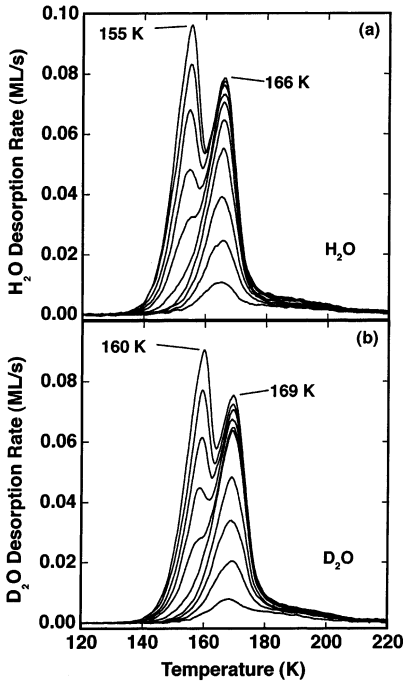

Figure 1. TPD spectra of H_2O (a) and D_2O (b) from FeO(111) for a range of initial coverages (0.2, 0.4, 0.6, 0.8, 1.0, 1.2, 1.4, 1.6, 1.8, and 2.0 ML). The water was deposited at 80 K and the heating rate was 1 K/s.

taken under similar conditions for H_2O and D_2O on Pt(111) (data not shown) yield similar peak separations of 12 K for H_2O and 10 K for D_2O. The monolayer peak for D_2O on FeO-(111) is shifted to higher temperature by about 3 K relative to H_2O. A kinetic analysis of the monolayer desorption, performed as described previously,[23,35] yields first-order desorption kinetics of $\nu = 10^{13.7\pm1}$ s^{-1}, $E_a = 46 \pm 2$ kJ mol^{-1} for H_2O and $\nu = 10^{14.0\pm1}$ s^{-1}, $E_a = 48 \pm 2$ kJ mol^{-1} for D_2O. Neither the monolayer nor the second layer of water on FeO(111) exhibit zero-order desorption as found on Pt(111). The first layer of water on Pt(111) desorbs with zero-order kinetics because of a two-dimensional two-phase coexistence between gaslike and condensed water phases.[42] A lower surface diffusion rate or a greater density of traps for diffusing water molecules on the FeO(111) surface might prevent the 2D water/FeO(111) system from achieving equilibrium between surface phases and could be the origin of this difference. The difference in the second layer may indicate that the structure of the monolayer is different from the structure of the terminated bulk so that water desorbing from the second layer does so from a different molecular configuration than found in the terminated bulk. The second layer may not form 2D islands on the first layer, or if it does similar considerations as for the first layer, may prevent a 2D phase equilibrium from becoming established. For initial water exposures 3 ML and greater, the leading edges of the TPD coincide as expected for zero-order multilayer desorption.

Figure 2 shows a set of D_2O TPD spectra for a sequence of initial D_2O exposures at 80 K from 5 to 20 ML. The spectra exhibit a common leading edge, characteristic of zero-order desorption from bulk water. For the 20 ML sample, there is a well-defined jog in the desorption line shape near 161 K. Below the jog, the desorption results from amorphous solid water and above it from crystalline water. This jog is a result of the difference in desorption rate between amorphous solid water (ASW) and crystalline ice (CI).[43,44] For progressively thinner samples, the jog resulting from crystallization shifts to successively lower temperatures. This demonstrates that over this range

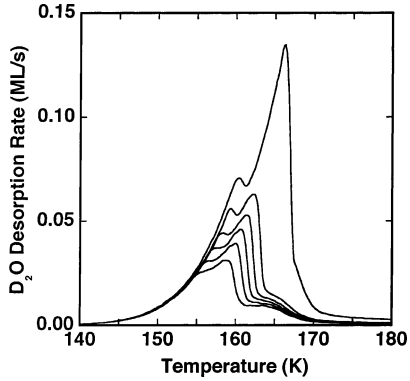

Figure 2. TPD spectra of D_2O from FeO(111) for a range of initial coverages (5, 6, 7, 8, 10, and 20 ML). The water was deposited at 80 K and the heating rate was 0.2 K/s.

of initial water coverage thin water layers crystallize more readily on FeO(111), similar to the behavior on Pt(111).[34] In contrast, an earlier publication reported that 5 ML of amorphous D_2O on FeO(111) was inhibited from crystallization.[32] The proposed origin of the suppression of crystallization was the weak interaction of water with the FeO(111) surface, which prevented heterogeneous nucleation of the crystalline phase. Our data are unable to address the location of the nucleation events. Recent work addressing the location of nucleation issue has concluded that on Ir(111) water films 150−1050 ML thick nucleate homogeneously in the bulk,[45,46] whereas on Pt(533), a 30 ML film nucleates at the water/vacuum interface.[47] The increased rate of crystallization for thin water films is not fully understood. However, the more facile crystallization realized for thin samples is inconsistent with an inhibited surface induced crystallization model.[32]

B. Infrared Spectroscopy. Figure 3 displays IRAS spectra for a sequence of water depositions at 30 and 135 K from 0.2 to 1 ML, with an additional spectrum for an 8 ML deposit. At all coverages and temperatures, the spectra exhibit a broad absorption between 2300 and 2700 cm^{-1}. The spectra at 30 K are similar to D_2O on FeO(111) IRAS spectra reported for water exposure at 110 K.[32] The observation of broad ν(OD) peaks in this region is considered a fingerprint of hydrogen bonding.[25] This broad absorption results from hydrogen bonding in water clusters or islands. The peak of this broad absorption feature is close to 2570 cm^{-1} for water coverages up to 1 ML at both temperatures. This is blue shifted from the 2550 cm^{-1} peak found at near monolayer coverage on Pt(111) for D_2O deposited at 25 or 140 K.[37,48] This feature exhibits a red shift for the 8 ML samples, by 18 cm^{-1} to 2552 cm^{-1} at 30 K and by 50 cm^{-1} to 2520 cm^{-1} at 135 K. At 30 K, the low coverage spectra have an overall line shape close to that found for the 8 ML amorphous water deposit, suggesting there is relatively little influence of the substrate on the hydrogen bonding between water molecules. The broad absorption band at low coverage and low temperature is in contrast to the sharper peaks found at 25 K for D_2O coverages $\leq$0.4 ML on Pt(111) which have previously been attributed to water monomers and hydrogen bonded dimers.[48] The general appearance of the submonolayer spectra at 135 K is very similar to submonolayer spectra for D_2O on Pt(111) deposited at 140 K.[37] There are subtle differences between the spectra for water adsorbed on FeO(111) at 30 and 135 K for coverages $\leq$0.4 ML. The low coverage spectra for the 30 K samples exhibit two small shoulders, one near 2650 cm^{-1} and one near 2500 cm^{-1}. The 2500 cm^{-1} feature is also found in the low coverage spectra

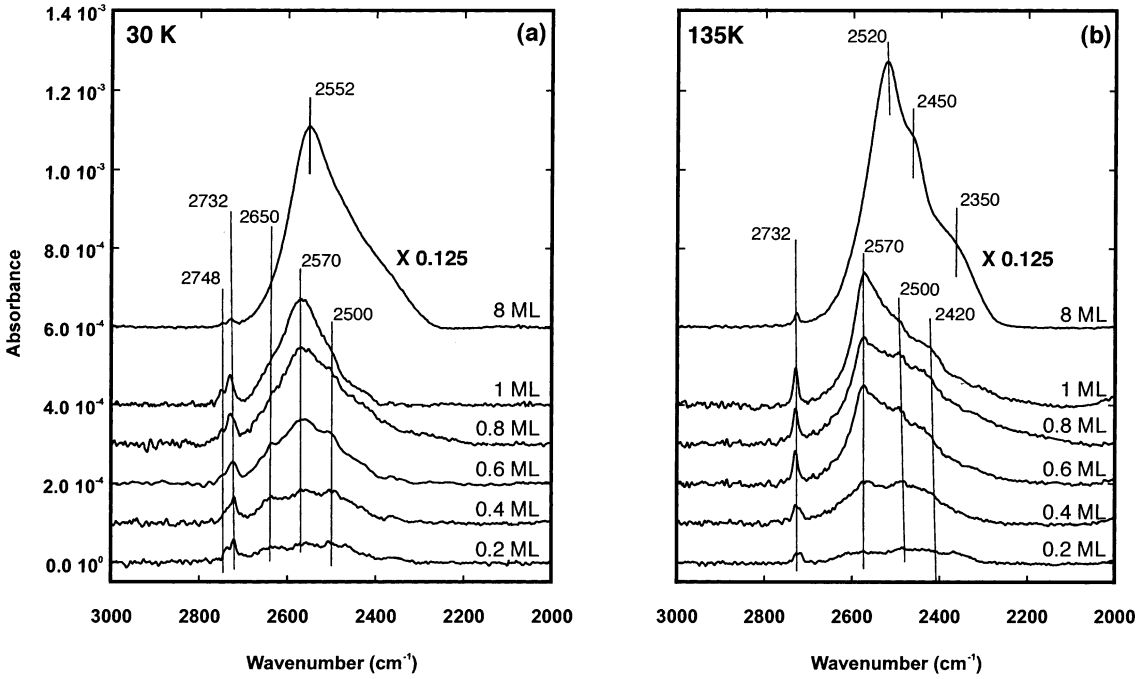

Figure 3. IRAS spectra of D_2O adsorbed on FeO(111) at 30 K (a) and 135 K (b) for a range of coverages (0.2, 0.4, 0.6, 0.8, 1.0, and 8 ML). The spectra were recorded at 30 K. The 8 ML spectra have been scaled by 1/8.

for the 135 K samples. The low coverage spectra for water adsorbed at 135 K have one additional feature, a small shoulder at 2420 cm^{-1}. At higher coverage, 1 and 8 ML, these small features are difficult to discern for the 30 K samples, whereas the features at 2500 and 2420 cm^{-1} appear to evolve into the red shifted shoulders at 2450 and 2270 cm^{-1} for the 135 K samples.

At higher coverages, 0.6 ML and greater, the broad absorption in the spectra for water deposited at 135 K differs from the spectra for the same water coverage deposited at 30 K. The peak position in the broad hydrogen bonded band is similar, ~2570 cm^{-1}, but the absorption falls off faster on the high-frequency side of this peak for water deposited at 135 K. The three features identified in the 0.2−1 ML, 135 K spectra at 2420, 2500, and 2570 cm^{-1} have red shifted counterparts at 2370, 2450, and 2520 cm^{-1} in the 8 ML 135 K spectrum. We expect D_2O deposited at 135 K to grow crystalline, and because the features in the 0.2−1 ML 135 K spectra evolve into corresponding features in the 8 ML crystalline spectra, we interpret the low coverage spectra as resulting from an ordered 2D D_2O layer on the FeO(111) surface. In contrast, the low coverage spectra for water adsorbed at 30 K appear similar to, and evolve into, the 8 ML amorphous spectrum, and we interpret the low coverage data as resulting from a disordered D_2O layer. These assignments will be further supported by N_2 TPD data discussed below.

The red shift in the peak IR absorption for the 8 ML films and the somewhat greater structure in the broad absorption at 135 vs 30 K are similar in character to what has been observed by other groups for ASW and crystalline H_2O thin films on a variety of substrates.[37,49−51] Similar spectral changes have also been observed after heating 25 ML of amorphous D_2O on FeO-(111) to 167 K.[32] Direct comparison of thin film IRAS data is difficult because differences in optical parameters (polarization, angle of incidence, film thickness, and density)[49] and differences in measurement temperature effect the spectra.[52] However, based on comparison of our spectra with those reported elsewhere,[37,49−51] we interpret the 8 ML film grown at 135 K to be predominantly crystalline D_2O. Although the differences in the monolayer and lower coverage infrared spectra are not dramatic, these data combined with the nitrogen TPD data discussed below suggests that for D_2O exposure up to a monolayer at 135 K there is ordering of the 2D overlayer.

In addition to the broad 2570 cm^{-1} absorption band there is also a weaker isolated spectral feature at 2732 cm^{-1}. It is sharper for water deposited at 135 K, and there is a shoulder near 2748 cm^{-1} for water deposited at 30 K. This feature grows with increasing coverage in a sub-linear fashion. Above 1 ML, in spectra not shown, it increases by 50% between 1 and 2 ML and by 30% between 2 ML and saturation near 4 ML. The peak at 2732 cm^{-1} has been attributed to the ν(OD) stretch of dangling OD bonds at the surface of a 2D or 3D ice island,[32] to water at the edge or interior of a 2D water island,[53] or to the uncoordinated OD bonds in the upper half of a bilayer.[37] The prominence of this feature, even at 0.2 ML, suggests that there must be a contribution to this feature from sites at the edges of 2D clusters or islands. This feature appears about twice as strong, relative to the broad hydrogen bonded band at 2570 cm^{-1}, on FeO(111) as for similar coverage spectra on Pt(111).[37] As we will show below, the mobility of water on FeO(111) at 30 K is low, and large, dense, 2D islands are not expected to be present at low coverage. Likewise, at low total coverage, the population in the second (and higher) water layer is small. Because of the higher binding energy for water molecules on the FeO(111) surface, 3D growth is not favored. Under such conditions, random deposition, possibly followed by a small number of diffusive steps, will result in a water surface structure consisting primarily of small islands or clusters with a high cluster edge to cluster interior ratio. The actual morphology of the clusters is unknown. It would be influenced by the energetics of all of the processes leading up to the establishment of pseudo-static structures. For instance, we presume the clusters would be different in shape if the diffusion rates were highly asymmetric with respect to direction on the surface. Given the constraint of a limited number of diffusion steps, it is not possible to form large, smooth, circular islands, i.e., structures which minimize the edge-to-surface ratio. The saturation of the dangling bond feature near 4 ML at both 30 and 135 K occurs

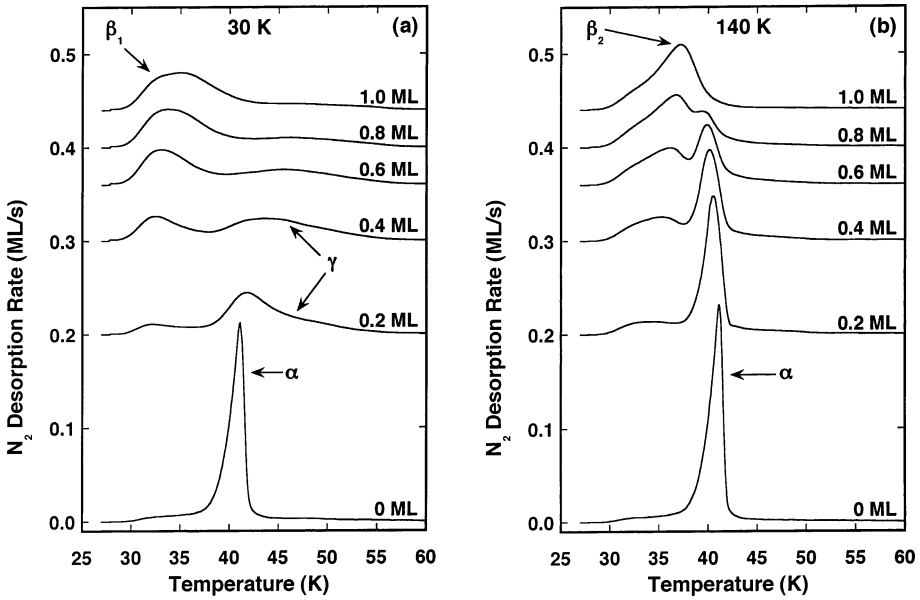

Figure 4. TPD spectra of N_2 from FeO(111) with various D_2O coverages (0, 0.2, 0.4, 0.6, 0.8, and 1 ML). The D_2O was deposited at 30 K (a) and 140 K (b). The heating rate was 0.5 K/s.

for thinner samples than in other IRAS measurements of D_2O on FeO(111) at 110 K.[32] One possible source of the discrepancy is that the background dosing employed in the earlier work led to some porosity of the sample which increased the total number of dangling bonds in thicker samples.[54]

The 2748 cm^{-1} shoulder in the 30 K spectra indicates there are different dangling bond environments at this temperature. We rule out the interpretation that this shoulder arises from D_2O monomers on the FeO(111) surface. On Pt(111) the highest frequency band found near 2706 cm^{-1} for D_2O deposited at 25 K has been attributed to monomers.[48] The sizable (42 cm^{-1}) blue shift required from Pt(111) to FeO(111) and the persistence of this band up through 8 ML makes interpreting this feature in a similar manner dubious. It must result from a local water bonding configuration which is not found in the ice grown at higher temperature. It is interesting to note that the D_2O deposition temperature effects the spectra in the dangling bond region somewhat independent of whether the contributing D_2O molecules are on or near the FeO(111) surface or well removed from it.

C. Nitrogen TPD. Figure 4 displays sets of N_2 TPD spectra taken on FeO(111) with various D_2O coverages from 0 to 1 ML. The features in the N_2 TPD are used as a probe of the water overlayer structure on FeO(111). The water was deposited at 30 and 140 K in Figure 4, parts a and b, respectively. The nitrogen was deposited at 28 K, slightly above the temperature required to condense N_2 multilayers,[23] and resulted in a single layer of N_2 on the D_2O/FeO(111) sample. The total nitrogen exposure was about two times greater than that required to saturate the monolayer features. There was no change in the TPD spectra for nitrogen exposures longer than that required to saturate the monolayer features. The nitrogen TPD spectrum from the bare FeO(111) surface exhibits a single sharp peak near 41 K (α) with a broad plateau below the sharp peak. The low-temperature plateau is a result of compression of the N_2 monolayer before growth of the second layer commences as found on clean Pt(111).[54,55] The α peak is close to zero-order, and in our previous study, we assigned this feature to desorption from terrace sites.[23] Defects (steps, kinks, or vacancies) in the FeO(111) surface result in a small amount of N_2 desorption at higher temperatures than the α peak. In our earlier work,[23] we used this higher temperature desorption on the bare FeO(111) surface to quantify the defect density, which was found to be ~0.11 ML. Comparison of the N_2 TPD spectra in Figure 4 with our earlier work indicates that the defect density here is somewhat smaller. We estimate the defect density from the relative area under the high-temperature portion of the spectra at ~0.07 ML.

Figure 4a shows there is a dramatic change in the nitrogen TPD after exposure to 0.2 ML of D_2O at 30 K. The sharp α peak is no longer observed, and now there is a broad desorption feature, γ, at higher temperatures ($T > 41$ K) and some increase in the desorption near 32 K (β_1). With successively higher D_2O exposure at 30 K, the β_1 peak grows in intensity and broadens while the γ peak decays in intensity. The nitrogen spectra after depositing D_2O at 140 K are substantially different from the 30 K spectra. After exposure to 0.2 ML of D_2O at 140 K, shown in Figure 4b, the α peak is reduced in intensity by about 50%, and there is some increase in intensity in the β_1 peak and the higher temperature γ peak. With successively higher D_2O exposure, the α and γ peaks are reduced in intensity and the low-temperature region evolves to a new peak near 37 K (β_2). It is still possible to see a small portion of the α peak for a water exposure of 0.8 ML, but there is no evidence of the α peak for a water exposure of 1 ML.

The difference between N_2 TPD spectra for the same water exposure, but different exposure temperatures, are substantial and in contrast to the subtle changes in the IRAS spectra shown in Figure 3. For example, compare the 0.4 ML IRAS spectra in Figure 3 with the N_2 TPD spectra for the same coverage in Figure 4. The IRAS spectra for different water adsorption temperatures are similar, with the same pair of small features, at 2570 and 2500 cm^{-1}, in the broad ν(OD) stretch spectral region and relatively subtle differences in line shape between the low and high-temperature spectra. In contrast, the N_2 TPD spectra for the same coverage are dramatically different. The N_2 TPD spectrum for water adsorbed at 30 K is substantially different from the spectrum for water adsorbed at 140 K for each of the identified peaks α, β_1, β_2, and γ. At 30 K, the N_2 TPD peaks associated with desorption from water covered regions on the FeO(111) surface grow in with increasing exposure as the β_1 peak, whereas at 140 K, it grows in as the

β_2 peak. Comparison of the N_2 TPD peaks associated with desorption from the FeO(111) surface shows that up to 1 ML coverage the α peak is lower in intensity and the γ peak is greater in intensity for water adsorbed at 30 vs 140 K. Understanding the origin of each feature will facilitate a description of the temperature-dependent behavior of water adsorbed on FeO(111).

The desorption temperature of a physisorbed atom or molecule is in general sensitive to the local structure of its adsorption site, although direct correlation with a particular site structure relies on correlation with other techniques and structural information. We assign the features in the N_2 TPD by comparison with other studies and plausible physical reasoning. The general appearance of the β_1 and β_2 peaks is qualitatively similar to monolayer nitrogen desorption from multilayers of ASW and CI reported earlier.[33,34] For multilayer water, it was found that the intensity of the N_2 desorption peak at 31.5 K decreased and the intensity of the desorption peak at 36 K increased relative to each other as the surface crystallinity increased.[34] By analogy with multilayer water, and supported by the difference in the IRAS peak shape for 1 ML of water deposited at 30 and 135 K in Figure 3, we assign the β_1 peak to desorption from a disordered water layer on FeO(111) and the β_2 peak to desorption from an ordered water layer on the same surface. We assign the γ peak to N_2 desorption from sites on the FeO(111) surface adjacent to adsorbed D_2O molecules. This is similar to the higher binding found for N_2 at defect sites on the FeO(111) surface.[23] If D_2O is immobile at low adsorption temperature then even at moderately low D_2O coverage a large fraction of N_2 adsorption sites on the FeO(111) surface will be adjacent to one or more D_2O molecules. Hence, the γ peak is expected to be prominent for these conditions. There are many possible D_2O configurations for N_2 adjacent to D_2O molecules on a partially covered FeO(111) surface, and we presume that the N_2 adsorbed at sites with higher D_2O coordination will have a higher binding energy resulting from a net increase in polarizability at the adsorption site. A broad range of configurational moieties will give rise to a broad N_2 desorption feature as observed in the γ peak, which extends from about 42 to 55 K. The α peak arises from N_2 adsorbed at FeO(111) terrace sites with no adjacent D_2O molecules as evidenced by the spectra from the bare FeO(111) surface. The α peak is distinguishable, with reduced intensity, as the D_2O coverage increases, for all submonolayer D_2O exposures at 140 K. This indicates there are areas not covered by D_2O on the FeO(111) surface of sufficient size that a substantial fraction of the N_2 adsorbed on, and in direct contact with, the FeO(111) surface is adjacent only to other adsorbed N_2 molecules. This can only result if a significant fraction of the adsorbed D_2O is clustered into relatively void free islands. The islands at 140 K must be primarily 2D because the α peak is no longer evident upon adsorption of 1 ML of D_2O, indicating there are no open patches on the FeO(111) surface, and there is negligible intensity in the γ peak, indicating there are very few voids in the D_2O monolayer.

The N_2 TPD spectra are able to distinguish three aspects of the local structure of water adsorbed on FeO(111). The β_1 and β_2 peaks reflect the local ordering of adsorbed water. Water is known to form ordered structures with hexagonal symmetry on close packed metal surfaces. Recent studies on Pt(111)[29] and Pd(111)[28] show the structure of molecularly adsorbed water may not always be the previously accepted bilayer structure.[24] The IRAS and N_2 TPD data are not able to discern the fine levels of structure, and we will not speculate on the details of the ordered water layer other than to consider it an ordered 2D layer. The α and γ peaks reflect the local structure of sites on the FeO(111) surface not covered with water. The α peak results from open regions on the FeO(111) surface with dimensions at least a few adsorbed N_2 cross-sections in two directions. The γ peak results from N_2 desorption from a site on the FeO(111) surface with at least one adjacent water molecule. The temperature and D_2O coverage dependence of the N_2 TPD peaks is a result of three processes. The first two are the surface diffusion rates of water on the FeO(111) surface and on water adsorbed on the FeO(111) substrate. These rates will primarily determine the intensities of the α and γ peaks. The other process is the 2D ordering of water islands or clusters. This process is not independent of the diffusion processes, but it is reasonable to envision the collective reordering, or relaxation, of a dense hydrogen bonded 2D water structure as distinct from the diffusive motion of individual water monomers or small clusters. We can further explore the temperature dependence of these processes, and the resulting water overlayer structure, with additional combinations of water exposure, deposition, and annealing temperatures.

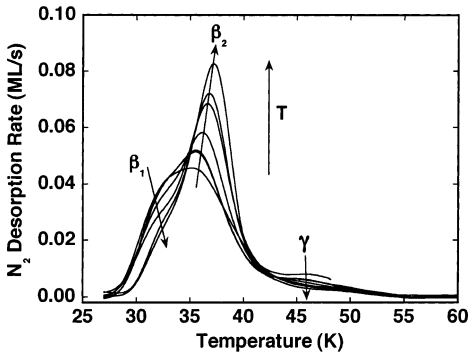

Figure 5. TPD of N_2 from FeO(111) with 1 ML D_2O deposited on the FeO(111) at 30 K. The D_2O has been annealed to 48, 80, 100, 120, and 140 K between successive N_2 TPD spectra.

Figure 5 displays a set of monolayer N_2 TPD spectra after depositing a monolayer of D_2O on FeO(111) at 30 K and then annealing to higher temperatures. As the annealing temperature is increased, the β_1 peak is converted to the β_2 peak associated with ordered 2D water islands. For annealing temperatures up through 80 K, there is increased intensity in the β_2 peak with very little change in the leading edge of the β_1 peak. Annealing above this temperature leads to a decrease in the β_1 peak concurrent with a further increase in the β_2 peak. Before annealing, there is some N_2 desorption from the γ peak, indicating that there are voids in the water overlayer leaving bare sites on the FeO(111) surface exposed. There is a substantial initial decrease in the γ peak intensity after annealing to 47 K with subsequent decreases occurring in a uniform manner with increased annealing temperature. The decay in the γ peak arises from small voids in the first layer of D_2O filling as water adsorbed on the second layer diffuses to, and binds at, a previously bare site on the FeO(111) surface. Initially there will also be some reduction in the γ peak associated with diffusion of water molecules with low coordination to sites with higher coordination, reducing the number of high coordination sites available for N_2 adsorption. We note that the final transformation of the β_1 peak to the β_2 peak occurs in a similar temperature range, 135−145 K, as that reported as a prerequisite to growing ordered water overlayers on Pt(111).[37,38]

To investigate the deposition temperature-dependent clustering of water on FeO(111), we performed nitrogen TPD experiments as a function of both water coverage and deposition

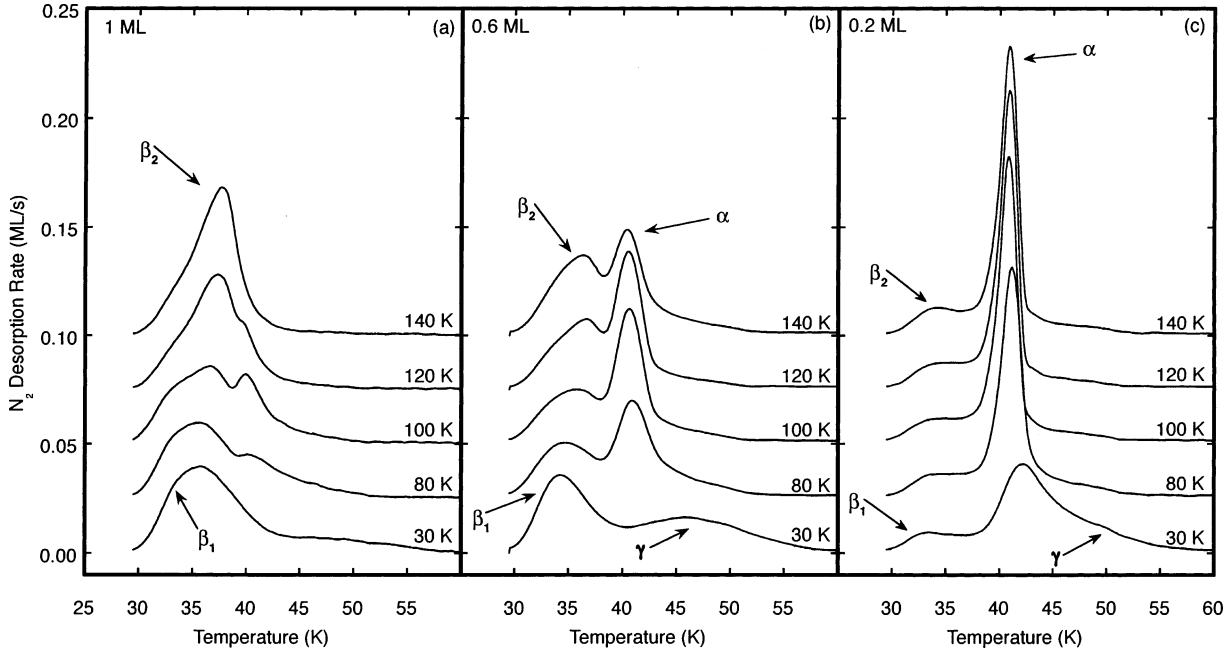

Figure 6. TPD spectra of N_2 from FeO(111) with preadsorbed D_2O for various D_2O deposition temperatures (T_{dep} = 30, 80, 100, 120, and 140 K) and coverages (1 ML (a), 0.6 ML (b), and 0.2 ML (c)). The heating rate was 0.5 K/s.

temperature. Figure 6 shows a sequence of D_2O adsorption temperature-dependent N_2 TPD spectra for initial water coverages of 0.2, 0.6, and 1 ML. The β_1 peak is prominent in the spectra for a 1 ML D_2O exposure at 30 K shown in Figure 6a. As the deposition temperature is increased, the β_1 peak is converted to the β_2 peak. At 30 K, there is also intensity in the γ peak, resulting from voids in the adsorbed water layer which exist because some water molecules are adsorbed in the second (or higher) water layer(s). As the water adsorption temperature is increased, there is a decrease in the high-temperature region of the γ peak, above about 46 K. Concurrent with this, for water deposited at 80 and 100 K, is an increase in the lower temperature region of the γ peak, below 46 K. This suggests that the average water coordination of N_2 on the FeO(111) surface decreases with increasing water adsorption temperature. A somewhat surprising behavior is found for the α peak. At 30 K, there is no resolvable α peak, but at 80, 100, and 120 K, there is clearly intensity in the α peak, which is no longer observed for water adsorbed at 140 K. This indicates that for the intermediate temperature range, 80−120 K, there are open areas on the FeO(111) surface large enough to support N_2 desorption from terrace sites. Since the total water coverage is the same for all spectra in Figure 6a, 1 ML, and enough to completetly cover the FeO(111) surface, the observation of the α peak indicates there is a fraction of the adsorbed water located in the second (or higher) layer(s) above the FeO(111) surface, even at 120 K. The N_2 desorption from terrace sites results from the adsorbed water clustering into dense 2D islands, leaving a substantial fraction of the bare FeO(111) sites as contiguous open regions. For this to happen, water must diffuse on the FeO(111) surface until it finds, and binds to, an existing water island. However, for open sites on the FeO(111) surface to remain open requires that much of the water in the second layer is unable to diffuse far enough to reach an unoccupied FeO(111) site. At 140 K, only the β_2 peak associated with an ordered D_2O monolayer on FeO(111) is observed. This indicates that at 140 K the water mobility on the adsorbed water layer is facile enough that all water molecules landing on the second layer diffuse to open sites on the FeO(111) layer below. The water adsorption temperature dependence can be successfully explained by a model in which water diffusion is more facile on the FeO(111) surface than on an adsorbed layer of water.

The spectrum for 0.6 ML of water at 30 K in Figure 6b has more intensity in the γ peak and less in the β_1 peak than the 1 ML spectrum at 30 K but similarly it does not exhibit a distinct α peak. At 80 K, the α peak is clearly resolved and the γ region intensity becomes reduced. The α peak becomes increasingly prominent for the depositions at 100 and 120 K, and the β_1 peak begins to evolve into the β_2 peak. The changes in the spectrum at 140 K are subtle with the α peak reduced slightly and slightly more intensity in the β_2 peak. For the 0.2 ML D_2O coverage spectrum in Figure 6c, the same trends are observed. However, at 30 K, there is considerably more intensity in the broad γ peak, in contrast to the spectra for higher D_2O coverage. This results from a surface with a sizable fraction of bare FeO(111) sites but a low density of terrace sites. At low total water coverage, 0.2 ML, but with the water randomly deposited, the uncovered FeO(111) sites will also be randomly arranged, and there will be very few large contiguous regions of the bare FeO(111) surface.

Using the N_2 TPD peak assignments given above, we can understand the spectra in the following way. In a pure hit-and-stick model, with zero mobility of water after adsorption, 1/e (0.37) of the FeO(111) surface would be uncovered after an exposure of 1 ML. This scenario would require a water molecule to adsorb on top of any existing water structure, including an isolated water monomer. This is physically unlikely, and we might expect that a water landing on an isolated water monomer would "fall off" onto an adjacent bare FeO(111) site. The resulting coverage in the first water layer will then be higher than the pure hit-and-stick model. For the purpose of illustration, we calculate site dependent adsorption on a square lattice. Using a square lattice, with zero mobility of the adsorbate, after depositing 1 ML, about 0.7% of the total surface would be open sites on the FeO(111) with no adjacent water molecules (terrace sites, α peak). For coverages of 0.2 and 0.6 ML, the fractions of similar sites are 37% and 5% respectively. It is more realistic to allow an incoming water molecule which lands on an existing water molecule, but with an immediately adjacent open site on the FeO(111) surface below, to move onto the open site. Water

molecules on the FeO(111) surface adjacent to another water are assumed immobile. Under these conditions, the fraction of terrace sites (α peak) will be 35%, 2.5%, and 0.07% for depositions of 0.2, 0.6, and 1 ML respectively, whereas the total fraction of open sites (α + γ peaks) will be 80%, 41%, and 14%. We consider the TPD spectra to arise from appropriately weighted fractions from the different adsorption sites, β, α, γ. If water deposited at 30 K had very low mobility on the FeO-(111) and water surfaces but could move downward to an adjacent open site, then the nitrogen TPD spectra for a coverage of 1 ML would have no FeO(111) terrace feature and have on the order of 10% higher binding sites for nitrogen on FeO adjacent to water (γ peak). Qualitatively, this is what is observed in the lowest temperature spectrum in Figure 6a. At 0.6 ML, the fraction of higher binding sites (γ peak) would be greater but the fraction of terrace sites might be too small, ∼2.5%, to observe. At 0.2 ML, there would be some desorption from terrace sites (α peak) and ∼80% of all desorption would be from sites on the FeO (α + γ peaks). Qualitatively this is what is shown in Figure 6, parts b and c.

To understand the spectra at intermediate temperatures, 80−120 K, shown in Figure 6, we consider the diffusion barrier for water on FeO(111) to be lower than on water adsorbed to the FeO surface. If water had some mobility on the FeO(111) surface at 80 K but very little on the water surface, then impinging water molecules landing on the FeO(111) surface could diffuse. If a diffusing molecule reached an existing water island or cluster, it would preferentially bind there. Water landing on an existing water island would in many cases not diffuse far enough to reach the edge of the island and bind to the FeO(111) surface. Under these conditions, the fraction of bare FeO(111) sites that are terrace sites would increase, whereas the total fraction of bare FeO(111) sites might not increase significantly. In the limit of zero mobility on the water surface and facile mobility on the FeO(111) surface, the fraction of bare FeO(111) would increase slightly under the proposed model. The fraction of water landing on water adjacent to a bare site would decrease as a consequence of the reduction in the edge-to-surface ratio for large islands. The TPD spectra for these temperatures would be expected to show an increase in the terrace site desorption feature, α peak, and a reduction in the highest temperature spectra, γ peak, a result of the reduced edge-to-surface ratio. Qualitatively, this is what is shown in Figure 6 for all coverages in the intermediate temperature range.

As the deposition temperature is increased, the diffusion rates of water on water and on FeO(111) will both increase. As evident from the TPD spectra in Figure 1, water binds more strongly to FeO(111) than to itself. We expect then that a water molecule which diffuses to the edge of a water island adjacent to an open site on the FeO(111) will move to the higher binding site on the FeO(111) surface. With sufficient water mobility on both surfaces, the water will wet the FeO(111) surface, filling the surface as a 2D structure before growing the second layer. For a deposition of 1 ML, there will be no bare FeO(111) regions remaining, as shown in Figure 6a, whereas for lower coverage, the total bare FeO(111) fraction (α + γ peaks) will decrease to the complement ($1 - \Theta_w$) of the first layer water coverage (Θ_w). The line shape for nitrogen desorption from the water islands shifts to higher temperature and β_1 transforms to β_2 above 120 K, similar to the annealing induced transforation shown in Figure 5. This change in the N_2 TPD line shape is similar to what is observed for nitrogen desorption from multilayer amorphous and crystalline water on Pt(111).[33,34] In analogy with this, we associate the shift from β_1 to β_2 with the two-dimensional ordering of the water layer.

The data in Figure 6 indicate that the diffusion of water on FeO(111) is more facile than for water on 2D water islands. Water appears to become sufficiently mobile on the FeO(111) surface near 80 K that on the timescale established by reciprocal of the deposition rate, ∼2 s, it can diffuse to, and bind to, an existing water cluster before another water lands on or adjacent to it. This temperature is about 10 K higher than determined for water diffusing on Pt(111) using a similar water flux.[42] The higher temperature suggests that the corrugation in the surface potential is greater on FeO(111) than on Pt(111). Work function changes upon adsorption of water on FeO(111) led Joseph et al. to conclude that initially water adsorbed on FeO(111) with the oxygen pointing down, leaving the hydrogens pointing up.[21] Although the proposed existence of isolated water monomers is not well supported in their later work[32] or in this study, the adsorption orientation may still hold. This would suggest that the water islands could in effect be hydrogen terminated. The stronger dangling bond ν(OH) signal, relative to water on the Pt(111) surface, is consistent with this interpretation. It is reasonable to consider that the corrugation of the potential energy surface for water on a hydrogen terminated surface is different than on an oxygen terminated surface.

IV. Conclusions

The adsorption of water on FeO(111) has been studied by TPD and IRAS as a function of deposition temperature and initial coverage. Water is found to desorb from FeO(111) molecularly with well resolved monolayer and multilayer peaks. Crystallization of thin films of water on FeO(111) becomes more facile with decreasing film thickness similar to the behavior on Pt(111) and other metal surfaces.[34] The IRAS measurements show that water is hydrogen bonded at low coverage at 30 and 135 K, and we find no evidence of isolated water monomers. At 30 K and low water coverage, the surface consists of small disordered D_2O islands or clusters. Differences in the surface corrugation between FeO(111) and an adsorbed water layer lead to water diffusing faster on the FeO(111) surface than the D_2O overlayer. For 1 ML of D_2O deposited below 120 K, the resulting film has voids, with some water adsorbed in the second layer. For water deposited above 120 K, ordered 2D islands are formed which completely wet the FeO(111) surface at saturation.

Acknowledgment. This work was supported by the U.S. Department of Energy, Basic Energy Sciences, Chemical Sciences Division. This work was performed at the W.R. Wiley Environmental Molecular Sciences Laboratory, a national scientific user facility sponsored by the Department of Energy's Office of Biological and Environmental Research and located at Pacific Northwest National Laboratory. Pacific Northwest National Laboratory is operated for the U.S. Department of Energy by Battelle under Contract No. DE-AC06-76RLO 1830.

References and Notes

(1) Schintke, S.; Messerli, S.; Pivetta, M.; Patthey, F.; Libioulle, L.; Stengel, M.; De Vita, A.; Schneider, W. D. *Phys. Rev. Lett.* **2001**, *87*.
(2) Kim, Y. D.; Wei, T.; Goodman, D. W. *Langmuir* **2003**, *19*, 354.
(3) Giordano, L.; Goniakowski, J.; Pacchioni, G. *Phys. Rev. B* **2003**, *67*.
(4) Campbell, C. T. *Surf. Sci. Rep.* **1997**, *27*, 1.
(5) Chambers, S. A. *Surf. Sci. Rep.* **2000**, *39*, 105.
(6) Freund, H. J.; Kuhlenbeck, H.; Staemmler, V. *Rep. Prog. Phys.* **1996**, *59*, 283.
(7) Goodman, D. W. *Chem. Rev.* **1995**, *95*, 523.

(8) Henry, C. R. *Surf. Sci. Rep.* **1998**, *31*, 235.
(9) Weiss, W.; Ranke, W. *Prog. Surf. Sci.* **2002**, *70*, 1.
(10) Weiss, W.; Barbieri, A.; Vanhove, M. A.; Somorjai, G. A. *Phys. Rev. Lett.* **1993**, *71*, 1848.
(11) SchedelNiedrig, T.; Weiss, W.; Schlogl, R. *Phys. Rev. B* **1995**, *52*, 17449.
(12) Weiss, W.; Ritter, M. *Phys. Rev. B* **1999**, *59*, 5201.
(13) Ritter, M.; Weiss, W. *Surf. Sci.* **1999**, *432*, 81.
(14) Ritter, M.; Ranke, W.; Weiss, W. *Phys. Rev. B* **1998**, *57*, 7240.
(15) Ranke, W.; Ritter, M.; Weiss, W. *Phys. Rev. B* **1999**, *60*, 1527.
(16) Roddatis, V. V.; Su, D. S.; Kuhrs, C.; Ranke, W.; Schlogl, R. *Thin Solid Films* **2001**, *396*, 78.
(17) Kim, Y. J.; Westphal, C.; Ynzunza, R. X.; Galloway, H. C.; Salmeron, M.; VanHove, M. A.; Fadley, C. S. *Phys. Rev. B* **1997**, *55*, 13448.
(18) Galloway, H. C.; Sautet, P.; Salmeron, M. *Phys. Rev. B* **1996**, *54*, 11145.
(19) Joseph, Y.; Ranke, W.; Weiss, W. *J. Phys. Chem. B* **2000**, *104*, 3224.
(20) Joseph, Y.; Kuhrs, C.; Ranke, W.; Ritter, M.; Weiss, W. *Chem. Phys. Lett.* **1999**, *314*, 195.
(21) Joseph, Y.; Kuhrs, C.; Ranke, W.; Weiss, W. *Surf. Sci.* **1999**, *435*, 114.
(22) Ranke, W.; Weiss, W. *Surf. Sci.* **1998**, *414*, 236.
(23) Liu, S. R.; Dohnalek, Z.; Smith, R. S.; Kay, B. D. *J. Phys. Chem. B* **2004**, *108*, 3644.
(24) Thiel, P. A.; Madey, T. E. *Surf. Sci. Rep.* **1987**, *7*, 211.
(25) Henderson, M. A. *Surf. Sci. Rep.* **2002**, *46*, 5.
(26) Morgenstern, M.; Muller, J.; Michely, T.; Comsa, G. *Phys. Rev. Lett.* **1997**, *198*, 43.
(27) Mitsui, T.; Rose, M. K.; Fomin, E.; Ogletree, D. F.; Salmeron, M. *Science* **2002**, *297*, 1850.
(28) Cerda, J.; Michaelides, A.; Bocquet, M. L.; Feibelman, P. J.; Mitsui, T.; Rose, M.; Fomin, E.; Salmeron, M. *Phys. Rev. Lett.* **2004**, *93*.
(29) Ogasawara, H.; Brena, B.; Nordlund, D.; Nyberg, M.; Pelmenschikov, A.; Pettersson, L. G. M.; Nilsson, A. *Phys. Rev. Lett.* **2002**, *89*.
(30) Michaelides, A.; Alavi, A.; King, D. A. *Phys. Rev. B* **2004**, *69*.
(31) Meng, S.; Wang, E. G.; Gao, S. W. *Phys. Rev. B* **2004**, *69*.
(32) Leist, U.; Ranke, W.; Al-Shamery, K. *Phys. Chem. Chem. Phys.* **2003**, *5*, 2435.
(33) Dohnalek, Z.; Ciolli, R. L.; Kimmel, G. A.; Stevenson, K. P.; Smith, R. S.; Kay, B. D. *J. Chem. Phys.* **1999**, *110*, 5489.
(34) Dohnalek, Z.; Kimmel, G. A.; Ciolli, R. L.; Stevenson, K. P.; Smith, R. S.; Kay, B. D. *J. Chem. Phys.* **2000**, *112*, 5932.
(35) Dohnalek, Z.; Kimmel, G. A.; Joyce, S. A.; Ayotte, P.; Smith, R. S.; Kay, B. D. *J. Phys. Chem. B* **2001**, *105*, 3747.
(36) Morgenstern, M.; Michely, T.; Comsa, G. *Phys. Rev. Lett.* **1996**, *77*, 703.
(37) Haq, S.; Harnett, J.; Hodgson, A. *Surf. Sci.* **2002**, *505*, 171.
(38) Glebov, A. L.; Graham, A. P.; Menzel, A. *Surf. Sci.* **1999**, *428*, 22.
(39) Braun, J.; Glebov, A.; Graham, A. P.; Menzel, A.; Toennies, J. P. *Phys. Rev. Lett.* **1998**, *80*, 2638.
(40) Su, X. C.; Lianos, L.; Shen, Y. R.; Somorjai, G. A. *Phys. Rev. Lett.* **1998**, *80*, 1533.
(41) Nordlund, D.; Ogasawara, H.; Wernet, P.; Nyberg, M.; Odelius, M.; Pettersson, L. G. M.; Nilsson, A. *Chem. Phys. Lett.* **2004**, *395*, 161.
(42) Daschbach, J. L.; Peden, B. M.; Smith, R. S.; Kay, B. D. *J. Chem. Phys.* **2004**, *120*, 1516.
(43) Smith, R. S.; Huang, C.; Wong, E. K. L.; Kay, B. D. *Surf. Sci.* **1996**, *367*, L13.
(44) Speedy, R. J.; Debenedetti, P. G.; Smith, R. S.; Huang, C.; Kay, B. D. *J. Chem. Phys.* **1996**, *105*, 240.
(45) Safarik, D. J.; Mullins, C. B. *J. Chem. Phys.* **2003**, *119*, 12510.
(46) Safarik, D. J.; Mullins, C. B. *J. Chem. Phys.* **2004**, *121*, 6003.
(47) Backus, E. H. G.; Grecea, M. L.; Kleyn, A. W.; Bonn, M. *Phys. Rev. Lett.* **2004**, *92*.
(48) Ogasawara, H.; Yoshinobu, J.; Kawai, M. *J. Chem. Phys.* **1999**, *111*, 7003.
(49) Mate, B.; Medialdea, A.; Moreno, M. A.; Escribano, R.; Herrero, V. J. *J. Phys. Chem. B* **2003**, *107*, 11098.
(50) Callen, B. W.; Griffiths, K.; Norton, P. R. *Phys. Rev. Lett.* **1991**, *66*, 1634.
(51) Bensebaa, F.; Ellis, T. H. *Prog. Surf. Sci.* **1995**, *50*, 173.
(52) Collier, W. B.; Ritzhaupt, G.; Devlin, J. P. *J. Phys. Chem.* **1984**, *88*, 363.
(53) Olle, L.; Salmeron, M.; Baro, A. M. *J. Vac. Sci. Technol. A* **1985**, *3*, 1866.
(54) Kimmel, G. A.; Stevenson, K. P.; Dohnalek, Z.; Smith, R. S.; Kay, B. D. *J. Chem. Phys.* **2001**, *114*, 5284.
(55) Kimmel, G. A.; Persson, M.; Dohnalek, Z.; Kay, B. D. *J. Chem. Phys.* **2003**, *119*, 6776.